Simulation of coherent radio pulses in air using the ZHS Monte Carlo

Juan Ammerman-Yebra,[a,*] **Jaime Álvarez-Muñiz**[a] **and Enrique Zas**[a]

Instituto Galego de Física de Altas Enerxías (IGFAE), Universidade de Santiago de Compostela, 15782 Santiago de Compostela, Spain

E-mail: juan.ammerman.yebra@usc.es

The well-known Zas-Halzen-Stanev (ZHS) Monte Carlo program, used to calculate coherent radio-pulses in dense media, has been extended to account for the deflections caused by the presence of a uniform magnetic field. This new development of the program can be used to simulate electromagnetic showers in constant density air. We compare results obtained to those of the ZHAireS program in the same conditions, and we explore the behavior of the frequency spectrum of pulses in air showers in a fairly generic way. By considering the effects in the generated pulses of different refractive indexes, densities and magnetic field intensities, it is possible to disentangle them and explain the main scaling properties of these showers, which are completely different from those in a dense medium such as ice. Finally the pulses obtained with ZHS for air at constant density are compared to those obtained with ZHAireS in a realistic atmosphere to demonstrate the validity and reach of the conclusions obtained.

*Speaker

1. Introduction

The study of coherent radio pulses emitted from air showers is a topic of increasing interest and activity. Although pulses from Ultra High Energy Cosmic Ray (UHECR) showers were studied in the 1960s [1] they were practically abandoned in the mid 1970s. The potential of the radio technique for neutrino detection in ice and the first code to simulate coherent radio pulses [2] revived the radio technique in the 1990s and lead to experimental initiatives such as ANITA [3]. The serendipitous discovery of GHz pulses from UHECR air showers with ANITA [4] together with other experiments [5] revived the radio technique for air showers in the 2000's. The first realistic simulations of coherent pulses in air were made in 2012 applying the technique developed for ice [2] to standard air shower simulation programs to obtain ZHAireS [6] and CoREAS [7], the current simulation standards using very similar algorithms [2, 8]. Progress has led to multiple initiatives for radio experiments in air to study UHECR showers and to search for UHE neutrinos.

The original ZHS, designed for ice, deals with electromagnetic interactions in homogeneous media neglecting magnetic effects. For this reason, it has not played a relevant role for studying showers in air except for testing purposes and to get coherent transition (TR) as a shower transits from ice to air [9]. The TR extension was used to disprove this type of showers could explain the "anomalous" events [10] detected with ANITA [11]. In this article we present a newly developed version of ZHS including the Lorentz force. This program allows simulation of pulses in air of constant density. Although it cannot reproduce realistic pulses in the atmosphere it can be used to calculate TR for UHECR showers in air that intercept the ice surface [12], an alternative explanation to the anomalous ANITA events [13], and to test the magnetic emission mechanism in the lab. It also allows the study of the effects of changing air density and magnetic field intensity in the radio pulse calculation and their relation to the shower properties.

2. Including the Lorentz force in the ZHS code

Particle tracks in ZHS simulations are defined between interactions (finer subdivisions are made when necessary). They are propagated in space including continuous energy loss and multiple elastic scattering and care is taken to account for the corresponding time delays. The ZHS code relies on an algorithm to calculate radio pulses[1] from each track. The charged particle trajectories in the track are assumed to be rectilinear and uniform for the radio calculation so that a simple expression can be used for each track contribution to the radio pulse. Details of the code and its different extensions can be found in [2, 14].

The magnetic field is included in ZHS considering that each charged particle track rotates in a plane perpendicular to its original direction. The rotation angle is calculated analytically assuming constant energy loss per unit length and the particle trajectory is approximated by an arc of a circle giving the right particle rotation from which time delays and particle displacements consistent with energy loss are obtained [15]. The shower code has been tested comparing the longitudinal and the lateral distributions of particles for different values of B to those obtained with ZHAireS (assuming a constant density medium). The agreement between them for the longitudinal development (allowing for a 20 g cm^{-2} shift in depth to match shower maxima) is better than 4%.

---

[1]also addressed as the ZHS algorithm

For the lateral distribution it ranges from 7% with $B = 0$ to 14% with $B = 5G$. The two programs also give compatible pulses at the level of $\sim 5\%$.

3.   Radio pulses in extensive air showers

The new version of the ZHS program is used to compare pulses for air of different densities, refractive indices and magnetic fields. Two mechanisms are known to contribute to radio pulses in air showers, the excess charge (Askaryan effect) and the transverse currents induced by the Earth's magnetic field, B, (geomagnetic effect). The latter dominates for pulses in the atmosphere which are expected to scale with the component of B perpendicular to the shower axis ($B_\perp$). Both the shower dimensions (governing the coherence) and the refractive index (that fixes the Cherenkov angle and plays a role in the pulse amplitude) depend on air density. The density changes as the shower develops and its value at shower maximum where most of the emission can be expected to come from, depends on zenith angle. There is evidence that the pulses are affected by air density and that the linear dependence on the magnetic field strength can be broken, but no comprehensive discussion of these effects is known[16–18]. Most of the simulations made are limited to the conditions of given experimental facilities and it is difficult to identify these effects because they are taking place simultaneously as the shower direction changes.

Pulses from showers are studied with the new program as each of these variables is independently changed. It is possible to separate the two main mechanisms because they have different polarization patterns. We consider for simplicity a shower that develops in the positive z axis with the magnetic field pointing in the positive x direction, so that the main transverse current is aligned with the positive y axis. We study the emission in the Cherenkov direction and in the Fraunhofer limit to maximize coherence. The observer is located in the xz plane. The geomagnetic component lies precisely along the y direction, while the Askaryan effect component lies in the xz plane, practically parallel to the x axis. We refer to this polarization as the $\tilde{x}$ polarization. This geometry is convenient as it allows separation of the Askaryan and geomagnetic contributions by respectively considering the two orthogonal polarizations $E_{\tilde{x}}$ and E_y.

Magnetic Field Intensity. We start by changing the magnetic field strength between $B = 0.25$ and $B = 8$ G. We take a reference value of $B_0 = 0.5$ G (typical for the Earth) and each case has $B = f_B B_0$ with $f_B = 0.5, 1, 2, 4, 8$ and 16. In addition we consider the value of $B = 0.094$ G at which the Askaryan and geomagnetic effects are approximately equal in magnitude. Air density, ρ, is kept constant at a reference value of $\rho_0 = 1.2 \ 10^{-3} \ \mathrm{g \, cm^{-3}}$ (at sea level) and the refractive index is assumed to be $n = 1.0003$. The electric field amplitudes E_y are compared in the left panel of Fig. 1. In the right panel the amplitude is divided by f_B to test the expected scaling as the Lorentz force is proportional to $B_\perp$. The scaling is very accurate for B up to 0.25 G, small deviations ($\sim 2\%$) can be seen for $B = 0.5$ G which become larger as B grows indicating that other effects are taking place. By looking at the time delay distributions it has been checked that fewer particles contribute coherently at a given shower depth as the magnetic field increases. Particles have shorter curvature radii and therefore they are more delayed relative to a front moving at the speed of light. The $E_{\tilde{x}}$ component does not change with B up to $B = 0.25$ G, but it gets progressively reduced for increasing B because of the same reason.
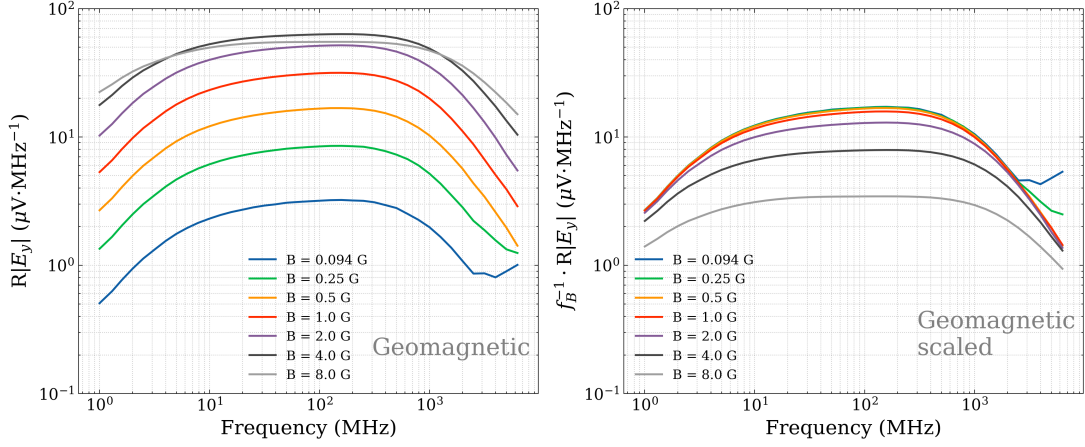
Figure 1: Average spectral amplitude of the E_y component of the radio pulse (geomagnetic effect) for 50 electron showers of 100 TeV moving in the z direction in air at sea level density for different magnetic fields B as labeled. The observer lies in the xz plane in the Fraunhofer limit and B points in the x direction. In the right panel the same amplitude has been divided by the scaling factor $f_B = B/B_0$ with $B_0 = 0.5$ G to display the scaling behavior and the deviations that appear when $B > 0.25$ G.

Density. The effect of density is studied in an analogous way comparing pulses with $\rho = \rho_0/f_\rho$ with $f_\rho = 1, 2, 4, 8, 16$. First we artificially keep the refractive index constant at the reference sea level value of 1.0003 and the magnetic field is set to $B = 0.5$ G. The results are shown in Fig. 2 for both the Askaryan and geomagnetic components. The plots on the left show the electric field amplitude. On the right the frequency is multiplied by f_ρ and the amplitude is divided by f_ρ in the geomagnetic case (E_y) to fully visualize the scaling properties. As the density is reduced by a given factor f_ρ all the tracks can be expected to increase in length because interactions depend on matter depth. As a result all shower dimensions in length and width and the corresponding time delays increase in proportion to f_ρ. Interference between particle tracks are responsible for the spectral features seen. A feature observed at frequency ν for the reference density ρ_0 appears at a shifted frequency ν/f_ρ when the density drops to ρ_0/f_ρ. Indeed when the amplitudes are plotted as a function of frequency multiplied by f_ρ the curves have the same dependence on the "x-axis" of the plot. The phase factor (given by frequency multiplied by the time delay) remains constant under this transformation. We also multiply the amplitude of the E_y component by f_ρ so that the behavior of the amplitudes as the density changes is very similar in the Askaryan and geomagnetic cases.

As the radio pulse is known to scale with tracklength [2] one can expect that the amplitude increases by the factor f_ρ due to the increased shower dimensions. This is indeed observed at low frequencies for the Askaryan component, $E_{\bar{x}}$ on the top left plot. The curves for density ρ_0 and $\rho_0/2$ indeed increase by a factor of two at the same frequency. On the top right plot they lie on top of each other because the curve for $\rho_0/2$ is shifted to the right (the frequency is multiplied by $f_\rho = 2$). The bottom right plot shows that the geomagnetic component increases by an extra factor of 2 for the same case; the amplitude must be reduced by f_ρ to display the same behavior as the Askaryan component. This can be understood because magnetic deflections are independent
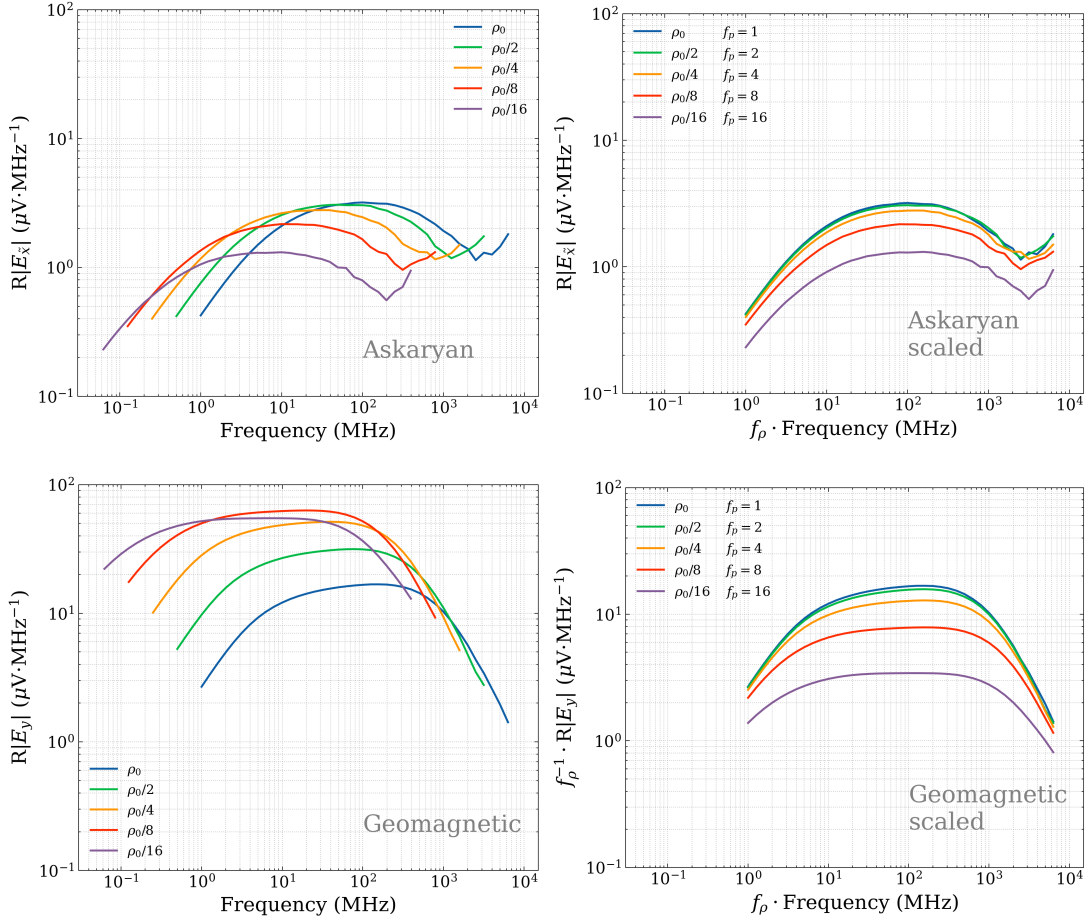
Figure 2: Average spectral amplitudes of radio pulses emitted in the Cherenkov direction of 50 showers in air at different densities as labeled. The refractive index $n = 1.0003$ is fixed and $B = 0.5\,\mathrm{G}$ points in the x direction. The set-up geometry and the showers are otherwise as described in Fig. 1. The Askaryan (geomagnetic) component, $E_{\tilde{x}}$ (E_y), is shown on the top (bottom). The raw spectra are plotted on the left while the same curves are shown on the right allowing for changes of the scales in both axes with the factor f_ρ as labeled (see text).

of density so that they remain the same when the density decreases and the shower dimensions increase accordingly. In other words, the curvature in the B field and the transverse currents become relatively more important compared to the shower dimensions as the density decreases. Once the scaling is accounted in this way for both components we see that for low values of f_ρ (high densities) the scaling is very good but it gets broken as the density drops by more than a factor of two. As the density decreases the time delays due to curvature are responsible for reducing the number of particles interfering coherently and deviations from the observed scaling become progressively more important, a feature that is common for both components.

The effect is not that different from that observed for changes of the magnetic field. Indeed, once these scalings have been accounted for, it is particularly revealing to note that the effect of increasing the magnetic field by a given factor is equivalent to reducing the density by the same factor. This is

shown explicitly in Fig. 3 for both the geomagnetic and Askaryan components. While increasing the magnetic field has the effect of reducing the curvature of the particles keeping the shower dimensions constant, decreasing the density keeps the curvature of the particles constant increasing the shower dimensions. If scaling factors are applied to eliminate the effect of changing the shower dimensions, the interference patterns will be controlled by the size of the curved trajectories relative to the shower dimensions. Similar effects can be achieved either reducing the curvature radii by increasing the B field, or increasing the shower dimensions by decreasing the air density.
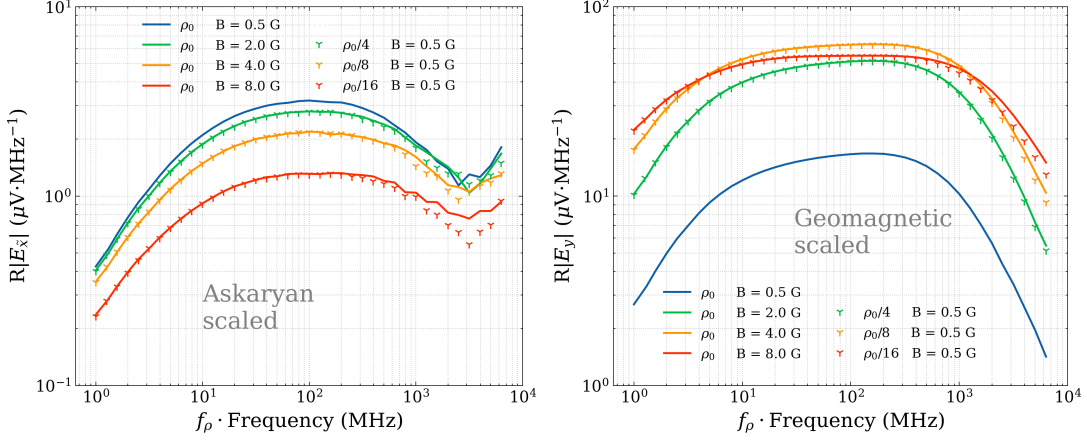

Figure 3: Average of the spectral amplitudes of the radio pulses of 50 showers initiated by a 100 TeV electron developing in air at different densities (with constant refractive index) and with different magnetic fields using the described scaling factors. The set-up geometry and the showers are otherwise as described in Fig. 1. The $E_{\tilde{x}}$ components are plotted on the left and the E_y components on the right. The frequency is multiplied by f_ρ to account for the change of scale of the showers.

In a realistic case the refractive index is coupled to density changes and its variation must be also taken into consideration. The Askaryan component is due to the longitudinal current carried by the excess charge of the shower front. The contribution is proportional to the projection of this current in a plane perpendicular to the observing direction assumed to make an angle θ to the shower direction. Observation at the Cherenkov angle, θ_C, implies that there is a projection factor given by $\sin\theta_C$. The refractivity, $n-1$, is typically assumed to be proportional to the air density ρ and it follows that $\sin\theta_C$ is proportional to $\sqrt{\rho}$. As a result, when the density is reduced the amplitude of the Askaryan contribution decreases in proportion to $\sqrt{\rho}$. The geomagnetic effect is practically independent because the transverse current is perpendicular to the shower direction and the projection factor, $\cos\theta_C$, is approximately 1 and hardly changes. Interference of the shower front particles is also proportional to $\sin\theta_C$ so that as the density is reduced it becomes less important and the high frequencies components of the electric field are enhanced. When density and refractive index are changed consistently the result is a superposition of the two effects. The net effect is shown on the left plot of Fig. 4 displaying the scaled version of the amplitude plot for the geomagnetic (E_y) component of the pulses. Further details can be explored in [15]. The results obtained for air at constant density can be of relevance also for a shower developing in the atmosphere. We have compared the results of a shower simulated with ZHAireS injected in the atmosphere at 14.5 km altitude with zenith angle 85°, to a shower simulated with ZHS in air at a
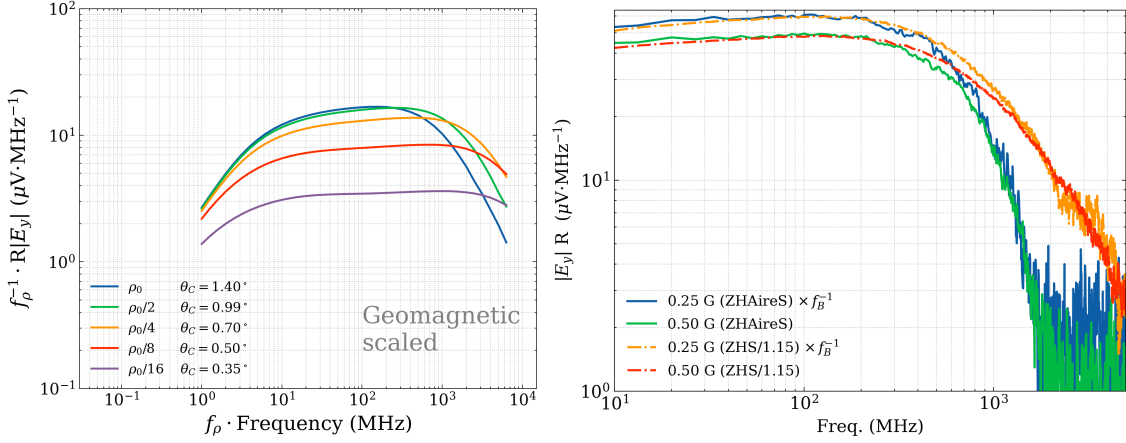
Figure 4: Left: Spectral pulse amplitude (E_y component) for consistent variations of ρ and n. The frequency and amplitudes are scaled with f_ρ as labeled. Right: Spectral pulse amplitudes (multiplied by distance to the observer) for two simulations of 100 TeV electron showers with ZHS in $\rho = 0.3 \, \mathrm{mg \, cm^{-3}}$ air compared to two with ZHAireS injected in the atmosphere at 14.5 km altitude at zenith angle 85°. In ZHAireS the observer is located at a position on the ground that approximately corresponds to the Cherenkov angle. The set-up geometry of the observer the shower and the magnetic field are kept otherwise as described in Fig. 1 in all cases. ZHAireS amplitudes have been multiplied by the distance to shower maximum and ZHS amplitudes have been divided by 1.15. Both $B = 0.25 \, \mathrm{G}$ and $0.5 \, \mathrm{G}$ are considered, Amplitudes for $B = 0.25 \, \mathrm{G}$ are divided by $f_B = 0.5$ to visualize deviations from linear scaling (see text).

constant density of $0.0003 \, \mathrm{gcm^{-2}}$, chosen to match the density of the atmosphere at the position of shower maximum for the ZHAireS simulation. For this zenith angle an observer located on the surface of the Earth is quite far away from the shower maximum approaching the Fraunhofer condition assumed in ZHS. The showers are started by 100 TeV electrons and the reference magnetic field intensity $B_0 = 0.5 \, \mathrm{G}$ is compared to $B = B_0 f_B = 0.25 \, \mathrm{G}$ for $f_B = 0.5$ (possible values of $B_\perp$ at many locations), consistent with the geomagnetic field at the Earth's surface. The simulation geometry is otherwise kept consistent with that discussed above. The results are shown in the right plot on Fig. 4 that displays the spectrum of E_y times the distance to shower maximum. It can be seen that the E_y spectra for both simulations agree in shape up to about 700 MHz, (above typical bandwidths in experimental setups). The different density profile used in ZHAireS could be responsible for deviations above 700 MHz. At low frequencies the amplitudes of the ZHS are only 15% higher than those of ZHS. In the comparison plot the ZHS amplitudes are divided by 1.15 to match the low frequency results of the two programs. In addition, the amplitudes in the plots for $B = 0.25$ in both simulations have been divided by $f_B = 0.5$ to correct for the assumed linear scaling with B. We appreciate that the scaling is not perfect and the pulses with $B = 0.5 \, \mathrm{G}$ are 22% below. What is most remarkable is that the same scaling violation is observed in both programs.

4. Conclusions

We have included magnetic deviations in the ZHS code, testing it against ZHAireS. The new program gives realistic simulations of coherent radio pulses in constant density air. We have studied

the effects of changing the magnetic field intensity and the air density and investigated the changes produced in the frequency spectrum of the pulses. By applying scaling laws to the frequency and the amplitude it has been shown that the behavior of the pulses is rather similar in all cases. The applied scaling laws are interpreted in terms of changes of the shower dimensions and particle delays including those associated to magnetic deflections. Simulations made with ZHAireS in the atmosphere indicate that the ZHS pulses studied in constant density display realistic features. These simulations show that deviations from the scaling behavior can be relevant for showers developing in low enough densities such as very inclined UHECR or stratospheric showers.

References

[1] J. V. Jelley, J. H. Fruin, N. A. Porter, T. C. Weekes, F. G. Smith and R. A. Porter, *Radio Pulses from Extensive Cosmic-Ray Air Showers*, *Nature* **205** (1965) 327.

[2] E. Zas, F. Halzen and T. Stanev, *Electromagnetic pulses from high-energy showers: Implications for neutrino detection*, *Physical Review D* **45** (1992) 362.

[3] P. Miocinovic, S. W. Barwick, J. J. Beatty, D. Z. Besson, W. R. Binns, B. Cai et al., *Tuning into UHE Neutrinos in Antarctica - The ANITA Experiment*, *ECONF C041213:2516,2004* (2005) [astro-ph/0503304].

[4] ANITA collaboration, *Observation of Ultra-high-energy Cosmic Rays with the ANITA Balloon-borne Radio Interferometer*, *Phys. Rev. Lett.* **105** (2010) 151101 [1005.0035].

[5] H. Rottgering, *LOFAR, A New low frequency radio telescope*, *New Astron. Rev.* **47** (2003) 405 [astro-ph/0309537].

[6] J. Alvarez-Muniz, W. R. Carvalho, Jr. and E. Zas, *Monte Carlo simulations of radio pulses in atmospheric showers using ZHAireS*, *Astropart. Phys.* **35** (2012) 325 [1107.1189].

[7] T. Huege, M. Ludwig and C. W. James, *Simulating radio emission from air showers with CoREAS*, *AIP Conf. Proc.* **1535** (2013) 128 [1301.2132].

[8] C. W. James, H. Falcke, T. Huege and M. Ludwig, *General description of electromagnetic radiation processes based on instantaneous charge acceleration in 'endpoints'*, *Phys. Rev. E* **84** (2011) 056602 [1007.4146].

[9] P. Motloch, J. Alvarez-Muñiz, P. Privitera and E. Zas, *Transition radiation at radio frequencies from ultrahigh-energy neutrino-induced showers*, *Phys. Rev. D* **93** (2016) 043010 [1509.01584].

[10] ANITA collaboration, *Characteristics of Four Upward-pointing Cosmic-ray-like Events Observed with ANITA*, *Phys. Rev. Lett.* **117** (2016) 071101 [1603.05218].

[11] P. Motloch, J. Alvarez-Muñiz, P. Privitera and E. Zas, *Can transition radiation explain the ANITA event 3985267?*, *Phys. Rev. D* **95** (2017) 043004 [1606.07059].

[12] J. Ammerman-Yebra, J. Alvarez-Muñiz and E. Zas, *Transition radiation and the anomalous events of ANITA*, *PoS* **ICRC2023** (2023) 1155.

[13] K. D. de Vries, A. M. van den Berg, O. Scholten and K. Werner, *Coherent Cherenkov Radiation from Cosmic-Ray-Induced Air Showers*, *Phys. Rev. Lett.* **107** (2011) 061101 [1107.0665].

[14] J. Alvarez-Muñiz and E. Zas, *Progress in the Simulation and Modelling of Coherent Radio Pulses from Ultra High-Energy Cosmic Particles*, *Universe* **8** (2022) 297.

[15] J. Ammerman-Yebra, J. Alvarez-Muñiz and E. Zas, *Density and magnetic intensity dependence of radio pulses induced by energetic air showers*, *arXiv preprint arXiv:2305.11668* (2023) .

[16] A. Romero-Wolf, *Radio Simulations of Upgoing Extensive Air Showers Observed from Low-Earth Orbit*, *PoS* **ICRC2021** (2021) 1031.

[17] C. Glaser, M. Erdmann, J. R. Hörandel, T. Huege and J. Schulz, *Simulation of Radiation Energy Release in Air Showers*, *JCAP* **09** (2016) 024 [1606.01641].

[18] S. Chiche, C. Zhang, K. Kotera, T. Huege, de Vries K., F. Schl uter et al., *New features in the radio-emission of very inclined showers*, *PoS(ARENA2022)035* (2023) .